Chemical Science

Cite this: *Chem. Sci.*, 2012, **3**, 1169

www.rsc.org/chemicalscience

EDGE ARTICLE

Heterometallic Cu^{II}/Dy^{III} 1D chiral polymers: chirogenesis and exchange coupling of toroidal moments in trinuclear Dy_3 single molecule magnets†‡

Ghenadie Novitchi,[a] Guillaume Pilet,[a] Liviu Ungur,[bc] Victor V. Moshchalkov,[d] Wolfgang Wernsdorfer,[e] Liviu F. Chibotaru,*[b] Dominique Luneau*[a] and Annie K. Powell*[fg]

Received 27th September 2011, Accepted 25th December 2011
DOI: 10.1039/c2sc00728b

The first example of exchange coupling between the toroidal moments in chiral heterometallic Cu^{II}/Dy^{III} 1D polymers built from alternating trinuclear Dy_3 SMM-building blocks and chiral copper(II) complexes is reported. A very strong toroidal magnetization can be induced by applying a magnetic field at low temperature in single-crystals of these compounds.

Introduction

Recent years have witnessed a burgeoning interest in applying coordination chemistry principles, based on the pioneering work of A. Werner,[1] to address the challenge of synthesizing tailored materials based on open shell metal ions. One particularly fruitful area which utilizes the electronic properties of collectively coupled paramagnetic entities is that of molecular-based magnetism.[2] Looking back over the development of this area it can now be recognized that the coordination compounds targeted for such magnetically coupled systems are essentially constructed using the principles of supramolecular chemistry, in terms of 0D supermolecules and 1D chains, 2D sheets and 3D extended lattices.[3] These magnetic systems based on paramagnetic metal ions are most appropriately described in terms of metallosupramolecular chemistry and the levels of organization observed can be related to the structural hierarchies observed in biological systems. Perhaps one of the most obvious structural aspects within biomolecules is their inherent molecular chirality and this aspect is most easily recognized when looking at organic molecules as a result of the prochiral nature of tetrahedral carbon. We should note, however, that the actual requirement for chirality in a spatial system is the lack of any S_n symmetry (improper rotation or rotation/reflection) element. However, the metal ions can add at least two further aspects in terms of chirality. Firstly, the nature of the coordination sphere can invest the system with inherent chirality, as seen for "octahedrally" coordinated complexes with bidentate donor ligands which reduce the O_h symmetry to D_3 and impose a handedness on the system. This aspect is beautifully exemplified in the honeycomb chiral networks based on a *tris*-oxalato building block.[4] The second possibility of introducing "the fourth dimension" available to systems built of atoms, is to invoke time-reversal dependencies which will be the case in systems with magnetic spins. Now it is necessary to break Z_2 symmetry in order to induce magnetic chirality, which can be visualized as a non-coplanar arrangement of non-collinear magnetic moments on the metal sites. An additional qualitatively new effect offered by non-collinear magnetization is the possibility of *toroidal magnetization* in strongly anisotropic molecules and crystals.[5,6c,d]

Our previously reported Dy_3 triangle[5d] can be regarded as the archetype of the non-collinear Ising antiferromagnetic arrangement seen in triangular lattices.[5a,c] Here the arrangement of antiferromagnetically coupled anisotropic spins have the easy axes essentially lying within the plane of the triangle and to fulfil the antiferromagnetic spin cancellation, these spins must be arranged at 120° to each other. The idea that "spin chirality" arises through having planar spins all pointing to the centre or all pointing away from the centre of the triangle,[5a] or alternatively the spins arranged at 120° to each other all going clockwise or anticlockwise around the triangle, is a misconception as a result of the requirement for the temporal aspect in magnetic systems.[6] Calculations have shown that in this particular case, the magnetic moments on Dy sites are slightly canted out of the plane of the triangle[5b] making the system truly chiral in magnetic terms. On the other hand, as calculations have shown,[5a,b] the

[a]*Université Claude Bernard Lyon 1, Groupe de Cristallographie et Ingénierie Moléculaire, Laboratoire des Multimatériaux et Interfaces, Campus de la Doua, 69622 Villeurbanne cedex. E-mail: luneau@univ-lyon1.fr*
[b]*Division of Quantum and Physical Chemistry, Katholieke Universiteit Leuven, Belgium. E-mail: Liviu.Chibotaru@chem.kuleuven.be*
[c]*INPAC-Institute for Nanoscale Physics and Chemistry, Katholieke Universiteit Leuven, Belgium*
[d]*Division of Solid State Physics and Magnetism, Katholieke Universiteit Leuven, Belgium*
[e]*Institut Néel, CNRS, Grenoble Cedex 9, France*
[f]*Institute of Inorganic Chemistry, Karlsruhe Institute of Technology, D76131 Karlsruhe, Germany. E-mail: annie.powell@kit.edu*
[g]*Institute of Nanotechnology, Karlsruhe Institute of Technology, Postfach 3640, D76021 Karlsruhe, Germany. E-mail: annie.powell@kit.edu*
† Electronic supplementary information (ESI) available. CCDC reference numbers 825779–825782. For ESI and crystallographic data in CIF or other electronic format see DOI: 10.1039/c2sc00728b
‡ Dedicated to Prof. Dante Gatteschi on the occasion of his 65th birthday.

ground state of each Dy_3 is characterized by an almost net toroidal moment, *i.e.* it is more properly described in terms of the recently recognised role of the toroidal spin structure, which is now regarded as one of the four possibilities invoked in multiferroic systems showing two or more out of ferroelectric, ferromagnetic, ferroelastic and ferrotoroidal behaviour.[6c,d] As a further illustrative example, we found that within a chiral supramolecular organisation of a duplex of three CuDy dinuclear units built into a chiral propeller motif, the huge anisotropy of the Dy^{III} ion is sufficient to display a similar arrangement of magnetic moments even though the individual Dy^{III} ions are quite remote from each other.[5e] The result of the system containing both structural enantiomers, and therefore both chiral arrangements of anisotropy axes on CuDy units, results in a dramatic change in hysteresis behavior on going from the dinuclear building block to the supramolecular propeller system.

Following on from these findings, we wanted to explore means of controlling molecular toroidal magnetization, which is an important direction towards the design of molecule-based multiferroics. Here we report the synthesis, structures, and magnetic studies of enantiopure heterometallic Cu^{II}/Ln^{III} 1D coordination polymers built from an alternation of the trinuclear Dy_3 SMM-building block and a chiral Cu^{II} *bis*-valinate complex which we constructed with the aim of propagating the chiral spin state along the chain.

Results and discussions

The reaction of *o*-vanillin (*HL*) and the respective enantiopure valine (**L** or **D**-*Val*) in methanol in a 1 : 1 molar ratio, followed by addition of $Cu(NO_3)_2\cdot 2.5H_2O$, and $Ln(NO_3)_3\cdot 6H_2O$ (Ln^{III} = Y(**L-1**), Dy(**L-2**,**D-2**), Gd(**D-3**)) yielded blue crystals suitable for single-crystal X-ray diffraction structure determination of general formula $\{[Cu(Val)_2CH_3OH][L_3Ln_3(\mu_3\text{-}OH)_2(NO_3)_4]\}_n$. IR spectra show that the compounds **1–3** are essentially identical both in the fingerprint region and the higher wavenumber region where the hydrogen-bonded O–H stretches lie, indicating that the three compounds are closely isostructural (Figure S1†). The enantiopurity of the complexes was confirmed by solid state circular dichroism (CD) spectroscopy (Figure S2†). The synthesis with racemic α-valine yielded the expected 1 : 1 mixture of crystals containing **L-2** and **D-2** as confirmed by single-crystal and powder X-ray diffraction. All complexes crystallize in the acentric monoclinic $P2_1$ space group. Enantiopurity was confirmed by refining Flack parameters to 0 (see Experimental section) giving 0.0, −0.01(2), 0.96(2) and 0.97(2) values for Y(**L-1**), Dy(**L-2**), Dy(**D-2**), Gd(**D-3**), respectively.

The crystal structures of the two ($\{CuDy_3\}_n$) 1D polymers **L-2** and **D-2** will be described first. **L-2** contains two independent chiral chains, **L-2-A(Δ)** and **L-2-B(Λ)**, in which alternating Dy^{III}_3 triangular building blocks and mononuclear Cu^{II} *bis*-**L**-valinate complexes can be observed. The trinuclear Dy^{III} units are capped by two μ_3-hydroxo centers and three deprotonated *o*-vanillin ligands which link pairs of Dy^{III} ions through the phenoxide groups. The aldehyde and methoxy groups of each ligand form 5 and 6 membered chelate rings (Fig. 1) with the same structural motif as observed previously for Ln_3 units when Ln = Dy^{III}, Gd^{III} and Tb^{III}.[5d,7]

Each Dy^{III} ion is 8-coordinated with a distorted geometry. For both chains, the Dy1/Dy11 and Dy2/Dy12 coordination environments are the same, being completed by one bidentate nitrate group and one carboxylate oxygen from the [Cu(**L**-*Val*)$_2$] unit, thus connecting Dy_3 triangles along the chains *via syn-anti* bridges. For the chain **A(Δ)**, the Dy13 environment is completed by one monodentate NO_3^- and the oxygen of a water ligand (Figure S3a†). In chain **B(Λ)**, the coordination sphere of Dy3 is completed by two NO_3^- groups in both mono- and bi-dentate coordination modes. The Dy^{III}–O bond lengths range from 2.29(1) Å to 2.72(1) Å (av.: 2.41 Å) and are in agreement with calculated BVS values (2.39 Å for Dy^{III}).[8] Within the [$Dy_3(\mu_3\text{-}OH)_2$] triangle units, the Dy···Dy distances are in the range 3.502(2)–3.538(2) Å. The shortest Dy···Cu intra-chain distances are 5.644(2) Å in chain **A(Δ)** and 5.732(2) Å in chain **B(Λ)**. The [Cu(**L**-*Val*)$_2$] bridge unit exhibits a square pyramidal structure with H_2O (chain **A(Δ)**) and methanol (chain **B(Λ)**) coordinated molecules in apical position.

In the case of **D-2**($\{CuDy_3\}_n$), **D**-valine was used in the synthesis instead of **L**-valine. The resulting structure is, as expected, a mirror image of that observed for **L-2** (Figure S3b†). In **D-2**, all bond lengths, distances and angles are comparable to those for the **L-2** complex: Dy^{III}–O bond lengths range from 2.29(1) Å to 2.72(1) Å (av.: 2.41 Å). Within the $\{Dy_3(\mu_3\text{-}OH)_2\}$ triangle units, the Ln···Ln distances are in the range 3.505(2)–3.543(2) Å and the shortest Dy···Cu intra-chain distances are 5.589(2) Å in chain **A(Δ)** and 5.573(2) Å in chain **B(Λ)**.

It should be stressed that the stereochemical aspects of chirality in the Dy_3 triangle (asymmetry) are induced by the linkage of Dy_3 triangle units by chiral Cu^{II} *bis*-valinate complex (Fig. 1). A similar triangular chiral topology can be observed for the organic molecule 1-chloro-2,2-dimethylaziridine,[9] and the relationship is pointed out in Fig. 1. Looking at the structural packing, it can be seen that for all complexes chains **A** and **B** run parallel to the *a*-axis of the unit-cell.

If we ignore the different details of the coordination environments of Dy3 and Dy13, then the chains A and B are related through a pseudo inversion centre. Strictly, however, as a result of the presence of either **L** or **D**-valine these compounds and their crystals have to be enantiopure as demonstrated by the CD and crystal structure determination. However, the crystal packing results in something close to an apparent racemic **Δ** and **Λ** arrangement of the main part of the chains (Fig. 1), thereby attenuating the effect of chirality.[1c,10]

The structure can be viewed overall as comprising planes of chains in the (*a*,*c*)-plane of the unit-cell. The shortest **A–A** and **A–B** intra-chain distances are 8.5 Å and the structural cohesion is provided by hydrogen-bonding interactions. The yttrium (**L-1**) and gadolinium (**D-3**) compounds are isostructural with **L-2** and **D-2**, respectively. X-ray data collection, refinement details, selected bond lengths and angles are given as supplementary materials (Table S1†). This set of compounds allows us to gauge the influence of the highly anisotropic Dy^{III} ion on the magnetic properties observed in **L-2** and **D-2** as explained below.

The thermal variation of the χT product for these $\{CuLn_3\}_n$ compounds under an applied magnetic field of 0.1 T is shown in Fig. 2 (**L-2**, **D-2**, **D-3**) and Figure S5† (**L-1**). For **L-1**, the $\{CuY_3\}_n$ complex, there is no contribution from the diamagnetic Y^{III} ion and the χT product at room temperature of

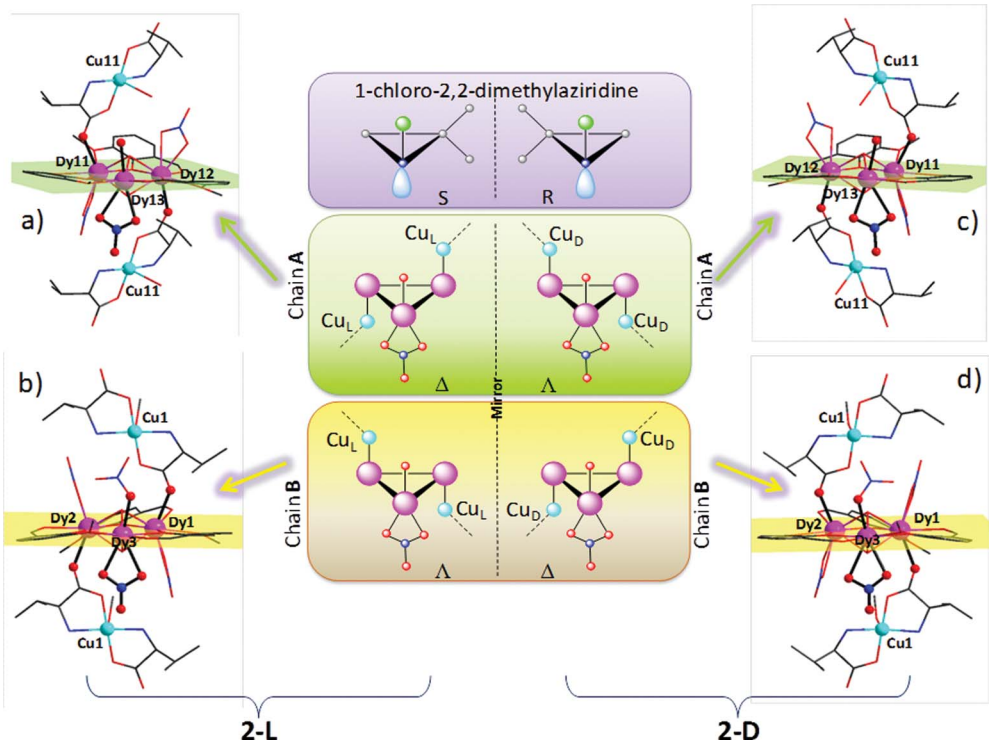

Fig. 1 Two chiral chains a) **L-2-A(Δ)** and b) **L-2-B(Λ)** in **L-2** compound, c) **D-2-A(Λ)** and d) **D-2-B(△)** in **D-2** compound. (In the middle) schematic representation of chiral Dy_3 units in **L-2** and **D-2** in comparison with organic analogue 1-chloro-2,2-dimethylaziridine.

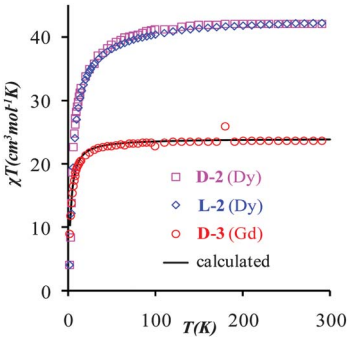

Fig. 2 Thermal dependence of the χT product per $CuLn_3$ unit at 0.1 T for **D-2**, **L-2** and **D-3**. The full lines correspond to the best calculated data (see text).

0.40 cm^3 K mol^{-1} is in excellent agreement with the calculated value of 0.398 cm^3 K mol^{-1} expected for four Cu^{II}, $S = ½$ with $g = 2.06$ and χT remaining constant over the temperature range as predicted for isolated non-interacting Cu^{II} ions. Compound **D-3** ($\{CuGd_3\}_n$) is isostructural with the **D-2** complex but the anisotropic Dy^{III} ions are replaced with isotropic Gd^{III} ions. At room temperature, the χT product (Fig. 2) is 23.65 cm^3 K mol^{-1} which is in a good agreement with the expected value of 24.02 cm^3 K mol^{-1} for three Gd^{III} ($^8S_{7/2}$ $S = 7/2$, $g = 2$) and one Cu^{II} ($S = ½$, with $g = 2.06$, using the values extracted from the analysis of **L-1**, the $\{CuY_3\}_n$ analogue.

On decreasing the temperature, the χT product decreases to reach the value of 8.90 cm^3 K mol^{-1} at 2 K, indicating the presence of dominant antiferromagnetic interactions. As a first approximation, the contribution to the magnetic interactions can be estimated using a simulation of χT and magnetisation curves from the simplest model with one repeating structural unit based on the following isotropic spin-Hamiltonian: $H = -2J_1S_1S_2 - 2J_2(S_2S_3 + S_3S_4 + S_2S_4)$.[11] In this case, $S_1 = ½(Cu^{II})$; $S_2 = S_3 = S_4 = 7/2$ (Gd^{III}) and J_1 and J_2 correspond to couplings for Cu-Gd and Gd-Gd interactions respectively. The variation of the Gd-Gd interaction (J_2) was restricted to lie between 0 and −0.3 cm^{-1} in line with values found in similar, previously reported, Gd_3 units.[7a]

This analysis led to $J_1 = -0.3 \pm 0.05$ cm^{-1}, $J_2 = -0.1 \pm 0.03$ cm^{-1} and $g = 2.0$ (Fig. 2 and S6†) which correspond to weak magnetic interactions for Gd-Gd as well as for Cu-Gd. For the *syn-anti* carboxylate-bridged Gd-Cu entity weak magnetic interactions are expected, with the sign depending on structural parameters and coordination environments and determining whether these can switch from ferromagnetic to antiferromagnetic.[12] In our case, a weak antiferromagnetic interaction is reasonable for the Cu-Gd interaction. The product of $\chi_M T$ for compound **L-2**($\{CuDy_3\}_n$), at $H = 0.1$ T, is 42.15 cm^3 K mol^{-1} at room temperature and decreases with decreasing temperature to reach 4.02 cm^3 K mol^{-1} at 2.0 K (Fig. 2). The value at room temperature is close to 42.91 cm^3 K mol^{-1} expected for three Dy^{III} ($^6H_{15/2}$, $L = 5$, $g = 4/3$)[13] and one Cu^{II} ($S = 1/2$, $g = 2.06$) ions. The experimental values of magnetization at 2 K and 5 K for **L-2**($\{CuDy_3\}_n$) are shown in Figure S7†.

Ac magnetic susceptibility measurements were performed in a 2–12 K range using a 2.8 G *ac* field in a 1–1000 Hz range for compound **L-2**($\{CuDy_3\}_n$) and are shown in Figure S9†. The temperature dependence of the in-phase susceptibility indicates

strong frequency dependence but without observable maxima, suggesting a low relaxation energy barrier. In the absence of an external *dc* field, the intensity of the out-of-phase signal observed for **L-2**($\{CuDy_3\}_n$) has a χ''/χ' ratio in the range 0.1–0.2, similar to that seen in the trinuclear Dy_3 SMM compound.[5d] Measurements performed under the application of a variety of low *dc* fields (Figure S9†) showed little change, suggesting that the relaxation mechanism of this SMM, at least above 2 K, is not influenced by quantum effects. The field evolutions of magnetization in **L-2**($\{CuDy_3\}_n$) are typical for cases where anisotropy is present and similar to previously reported values for triangular Dy_3[5a,c,d] SMMs and those based on modifications of the triangular motif.[14] The optical isomers in **D-2**($\{CuDy_3\}_n$) show very similar magnetic behaviour to that found in **L-2**($\{CuDy_3\}_n$) and the small differences are within experimental error limits of the magnetic measurements (Fig. 2 and S7†). For comparison and to aid in understanding the role of the Cu^{II} *bis*-**L**-valinate complex interacting with the Dy_3 SMM building block, micro-SQUID measurements were performed on single crystals of **L-2** and **D-2** (Fig. 3 and S10†). The profiles for the two enantiomers are broadly the same and the slight differences in detail are likely to be the result of small differences in the crystals used for the microSQUID measurements.

The *ab initio* calculations on the individual Dy^{III} and Cu^{II} magnetic sites in the **D-2** compound were performed within CASSCF/RASSI approach using the MOLCAS package[15a] and, in particular, the module SINGLE_ANISO,[5b,15b] which has recently been implemented in MOLCAS-7.6 (see SI† for computational details). The results for individual dysprosium centres are presented in Table 1. The main magnetic axes on Dy sites are close to tangential directions and lie almost in the plane of the Dy_3 triangle (Table 2 and Scheme 1) very similar to the arrangement of the main magnetic axes found in the ground state

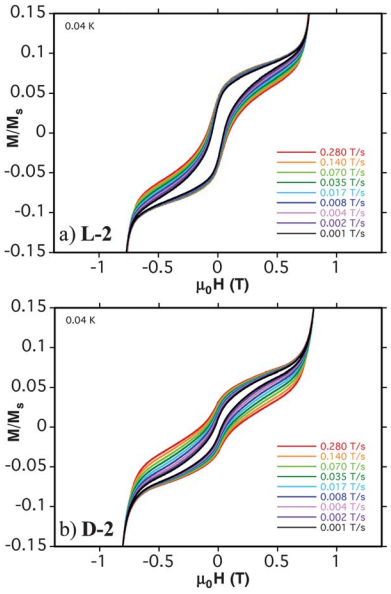

Fig. 3 Single-crystal magnetization (*M*) *vs.* applied field measurements for complex **L-2** (top) and **D-2** (bottom) with different field sweep rates at 0.04 K. *M* is normalised to its saturation value at 1.4 T. For temperature dependence data, see the supplementary materials†.

Table 1 Energies of the low-lying Kramers doublets (cm^{-1}) and main values of g tensors for the lowest Kramers doublet

	Dy1	Dy2	Dy3
	0.000	0.000	0.000
	89.773	94.571	118.074
	118.022	176.540	182.822
	164.407	227.134	229.912
	208.756	282.757	297.322
	307.808	338.063	343.775
	336.295	400.718	383.366
	423.123	560.323	430.332
	3551.928	3546.645	3560.904
	Main values of the *g* tensors		
g_x	0.0851	0.0323	0.0214
g_y	0.1107	0.0486	0.0298
g_z	19.5464	19.6482	19.6274

of the Dy_3 triangle[5a–c] showing that this motif is preserved despite the polymerization of Dy_3 units.

The exchange spectrum for the chains in **D-2** was simulated within the Lines model,[16] as discussed previously.[5b,15b,c] In the Lines model the exchange matrix is simulated by matrix elements of an effective isotropic exchange Hamiltonian written in the basis of low-lying spin–orbit multiplets on magnetic sites. In the present case the minimal model includes two Lines parameters J_1 and J_2 describing the Dy-Dy and Dy-Cu exchange interactions:

$$H_{Lines} = \sum_n \left[-J_1\left(\vec{S}_1^n \cdot \vec{S}_2^n + \vec{S}_2^n \cdot \vec{S}_3^n + \vec{S}_3^n \cdot \vec{S}_1^n\right) - J_2\left(\vec{S}^n \cdot \vec{S}_1^n + \vec{S}^n \cdot \vec{S}_2^{n+1}\right)\right] \quad (1)$$

where $S_1{}^n$, $S_2{}^n$ and $S_3{}^n$ are the spins $S = 5/2$ on Dy^{III} ions and S^n is the spin $S = 1/2$ on the Cu^{II} ion from the *n*-th unit cell (Fig. 1). The lowest multiplets on the metal ions, upon which the exchange Hamiltonian in eqn (1) is projected, are the spin doublet $S = 1/2$ on the Cu ion and the ground Kramers doublets on the Dy1, Dy2 and Dy3 ions. The latter are described by pseudospins $s_i = 1/2$, $i = 1,2,3$, at each unit cell of **D-2** chains, neglecting the exchange admixture of higher Kramers doublets on each Dy site due to their relatively high energies (see Table 1). Given the strong axiality of Dy sites ($g_{x,y}/g_z = 0.001$–0.006, see Table 1) the exchange interaction involving these multiplets reduces almost exactly to a *non-collinear* Ising model for projections (s_{i,z_i}) of pseudospins s_i on the corresponding anisotropy axis z_i (shown in Scheme 1). This exact mapping onto a non-collinear Ising model was recently found in dysprosium triangles,[5a,b] as well as in polynuclear complexes of other

Table 2 Orientations of the main magnetic axes for the lowest Kramers doublets on Dy sites in **D-2**

	Dy1	Dy2	Dy3
Angle of anisotropy axis with the tangential direction (φ)			
	10.3°	12.1°	15.6°
Angle of anisotropy axis with Dy3 plane			
	7.9°	0.1°	10.2°
Angle between the main anisotropy axes within the Dy3 triangle			
Dy1	—	121.7°	115.1°
Dy2	121.7°	—	123.2°
Dy3	115.1°	123.2°	—

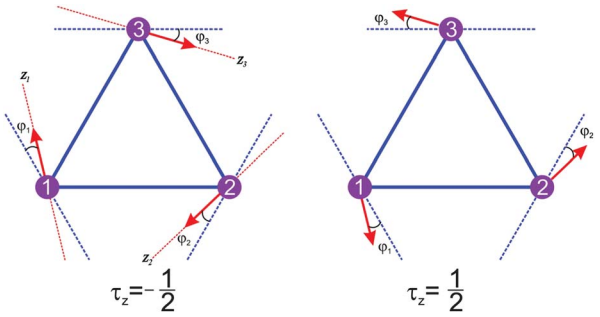

Scheme 1 Two components of the toroidal state $\tau = 1/2$ of the Dy_3 triangles. Blue dashed lines show the tangential directions and red dashed lines—the anisotropy axes on the corresponding Dy ions.

lanthanides.[17] On the other hand the interaction between strongly axial Dy^{III} ions and almost isotropic Cu^{II} ions reduces almost exactly to a *collinear* Ising model between the pseudospin projection s_{i,z_i} of Dy^{III} and the spin projection S_{z_i} of Cu^{II} taken on the same axis z_i (Scheme 1). This type of exchange interaction was also deduced for Cu–Dy pairs in 4f-3d-4d heterometallic chains.[15c] Thus the exchange interaction for **D-2** chains, involving the lowest Kramers doublets on metal sites, maps almost exactly onto the following Ising Hamiltonian:

$$\tilde{H}_{exch} = \sum_n \Big[-\tilde{J}_1 \left(s^n_{1,z_1} s^n_{2,z_2} + s^n_{2,z_2} s^n_{3,z_3} + s^n_{3,z_3} s^n_{1,z_1} \right) - \tilde{J}_2 \left(S^n_{z_1} s^n_{1,z_1} + S^n_{z_2} s^{n+1}_{2,z_2} \right) \Big] \quad (2)$$

where the index n denotes, as in eqn (1), the unit cell along the chain and the new exchange parameters are given by the expressions:[5a,18]

$$\tilde{J}_1^{i,i+1} = 25\cos\varphi_{i,i+1} J_1, \qquad \tilde{J}_2 = 5J_2 \quad (3)$$

where $\varphi_{i,i+1}$ are the angles between the anisotropy axes on Dy sites (Table 2). If we take $\varphi_{i,i+1} \approx 120^\circ$ we obtain $\tilde{J}_1 = -12.5 J_1$. Note that the energy spectrum of (1) is invariant under the change of sign of $\tilde{J}_2$.

The values of the best Lines exchange parameters, obtained from the fitting of $\chi T(T)$ and $M(H)$ for **D-2** are $J_1 = 0.47$ cm^{-1} and $J_2 = 0.64$ cm^{-1} The corresponding parameters in eqn (2) are $\tilde{J}_1 = 5.8$ cm^{-1} and $\tilde{J}_2 = \pm 3.2$ cm^{-1}. Fig. 4 shows the comparison of measured and calculated magnetic susceptibility and molar magnetization for **D-2**. (see also Figures S13–S15†). These simulations were done in full analogy with a previous treatment of mixed lanthanide–transition metal chains,[15c,19] without taking into account the inter-chain exchange interactions which are probably not important.

Due to the antiferromagnetic coupling between Dy ions ($\tilde{J}_1 > 0$), the local magnetic moments are arranged in a toroidal fashion (Fig. 5a, Scheme 1), as was the case in the previously investigated dysprosium triangle.[5] Furthermore, the obtained value for $\tilde{J}_1$ and other data in Table 1 allows us to conclude that the polymerization of the Dy_3 units has not changed their magnetic properties in any significant way. Indeed, as in the Dy_3 triangles, the three magnetic moments in the Dy_3 unit, having each *ca.* 10 μ_B, sum up into a small total moment ($\mu \approx 0.8\mu_B$ in the present case). Fig. 5b and 5c show that the uncompensated moments of

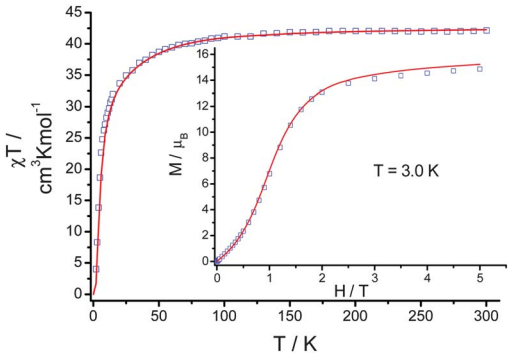

Fig. 4 A comparison between measured (empty squares) and calculated (red line) magnetic susceptibility for the **D-2** chain. Inset: a comparison of the measured and calculated molar magnetization at 3.0 K for the **D-2** chain.

Dy_3 units (μ) and the moments on the copper sites (μ_{Cu}) alternate antiferromagnetically along the chain resulting in zero magnetization of the ground state. Scheme 2a shows the projection of these moments on the plane perpendicular to the axis of the chain (Z).

The lowest excitation within one Dy_3 unit in the **D-2** chain, corresponding to the reversal of magnetic moment on the Dy3 site (the only one which is not connected with the neighbouring Cu ions, see Scheme 3), has the energy $\tilde{J}_1 = 5.4$ cm^{-1}. At the same time, the excitations not affecting the relative arrangement of s^n_{i,z_i} in each Dy_3 unit will be proportional to $\tilde{J}_2$and will lie, therefore,

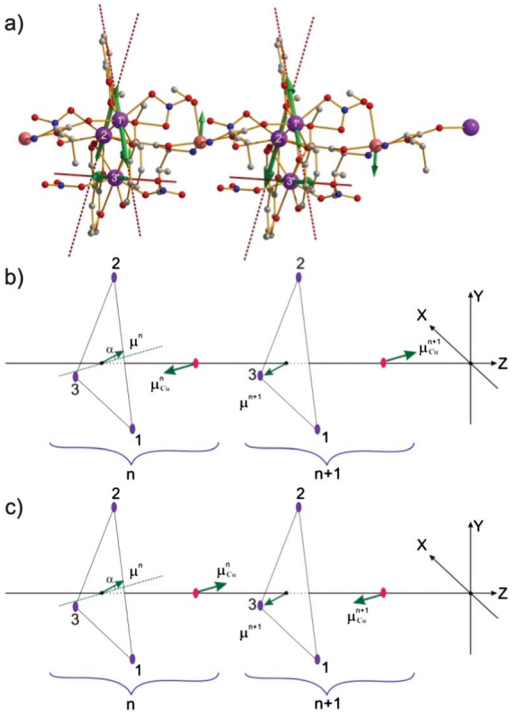

Fig. 5 Calculated anisotropy axes for the lowest Kramers doublets on Dy ions in the **D-2** chain. Green arrows show the orientation of the local magnetic moments in the ground state on Dy and Cu ions (a) and the uncompensated magnetic moments on each Dy_3 unit in the case of $\tilde{J}_2 > 0$ (b) and $\tilde{J}_2 < 0$ (c). α is the angle between μ^n and μ^n_{Cu}.

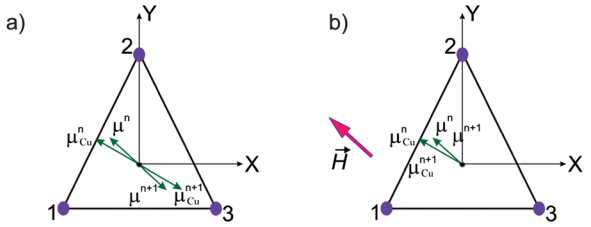

Scheme 2 View along the Z axis of μ and μ_{Cu} in the ground state of the **D-2** chain: a) $H = 0$; b) $H > H_c$ (see the text). Superscripts n and $n + 1$ denote nearest neighbour unit cells in a chain.

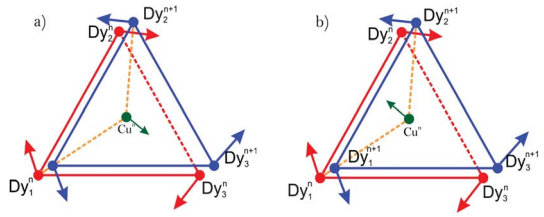

Scheme 3 Arrangement of the neighbouring toroidal moments in the case of a) antiferromagnetic Cu-Dy coupling ($\tilde{J}_2 > 0$); b) in the case of ferromagnetic Cu-Dy coupling ($\tilde{J}_2 < 0$).

lower in energy. For such excitations, the Dy_3 units are found in one of the toroidal magnetic states shown in Scheme 1, corresponding to toroidal quantum numbers $\tau_Z^n = \pm 1/2$.[20] These states are characterized by a *toroidal* magnetic moment,[6c,20] which simply corresponds to the torque of magnetic moments on Dy^{III} ions measured from the centre of the corresponding Dy_3 triangle (Scheme 1) and being, therefore, a vector directed almost perpendicular to its plane. The Hamiltonian describing these low-lying states is obtained from eqn (2) by allowing only for the toroidal states (Scheme 1) on all Dy_3 units of a **D-2** chain. For such states the term proportional to $\tilde{J}_1$ in eqn (2) is always a constant equal to $-\tilde{J}_1(1/2 \times 1/2 \times 3) = -3/4\tilde{J}_1$. Since in the toroidal states the directions of magnetic moments on all three Dy sites are fully determined by the value of the corresponding toroidal quantum number τ_Z (see Scheme 1), we can replace in the second term of eqn (2) the spin projection operators s^n_{i,z_i} by the toroidal momentum operators τ^n_Z of the corresponding unit cell n. Thus the Hamiltonian describing the low-lying excitations in **D-2** chains has the form:

$$\hat{H}_{LL} = \sum_n \left[-\frac{3}{4}\tilde{J}_1 - \tilde{J}_2\left(S^n_{z_1}\tau^n_Z + S^n_{z_2}\tau^{n+1}_Z\right)\right]. \qquad (4)$$

Eqn(4) describes the Ising interaction between toroidal and spin moments along the chain. The lowest excitations described by this Hamiltonian correspond to the creation of one domain wall (soliton), when starting with some Cu or Dy_3 unit all moments to the right of it are reversed in the chain. Supposing that the anisotropy axes on Dy ions are exactly at 120° to each other (see Table 2), the energy of this excitation becomes $E_{soliton} = \frac{\sqrt{3}-1}{4}|\tilde{J}_2| \approx 0.59$ cm^{-1}. The next low-lying excitations correspond to the reversal of one moment in Fig. 5b and 5c and have the energies:

$$E(\mu^n \rightarrow -\mu^n) = \frac{\sqrt{3}-1}{2}|\tilde{J}_2| = 1.18 \text{ cm}^{-1}$$
$$E(\mu^n_{Cu} \rightarrow -\mu^n_{Cu}) = \frac{\sqrt{3}}{2}|\tilde{J}_2| = 2.77 \text{ cm}^{-1} \qquad (5)$$

We can see that the lowest excitation of this type involves the reversal of the toroidal moment τ_Z (and the accompanying reversal of the uncompensated magnetic moment μ) on one of Dy_3 units.

The magnetic structure in Fig. 5 shows no bulk toroidal magnetization. This is because the toroidal moments in the neighbouring Dy_3 units are opposite in sign and compensate each other. Indeed, looking at a given triangle with a given arrangement of Dy spins will reveal opposite rotation of the spin picture depending on whether this is viewed from the front or the back. This is exactly the effect produced when viewing a modern wind turbine from the front or the back—if the front view has the blades turning clockwise, from the back they will appear to be rotating anticlockwise although the physical structure remains the same. Furthermore, we stress that the antiferromagnetic arrangement of the toroidal moments in the ground state does not depend on the sign of the exchange interaction between Cu and Dy. Indeed, Fig. 5c shows that the same antiferromagnetic ordering of toroidal moments can be generated by both ferromagnetic and antiferromagnetic interaction between Cu^n and its neighbors $(Dy1)^n$ and $(Dy2)^{n+1}$. The only reason for the antiferromagnetic arrangement of the toroidal moments is the involvement of different types of Dy ion in the exchange pathway. The same antiferromagnetic arrangement of τ_Z would arise for couplings $(Dy1)^n$-Cu^n-$(Dy3)^{n+1}$, $(Dy2)^n$-Cu^n-$(Dy3)^{n+1}$ (where n denotes the unit cell in which a given segment is situated) and so forth. In contrast, for exchange geometries involving Dy ions of the same type, *e.g.* $(Dy1)^n$-Cu^n-$(Dy1)^{n+1}$, the arrangement of toroidal moments will be of ferromagnetic type, irrespective of the sign of exchange interaction between Cu and Dy ions. In this latter case the ground state of the chain will be characterized by very strong magnetic chirality (*i.e.* by very large toroidal magnetic moment per unit cell). Synthesis of such chains is a challenging task for the future work.

Despite the lack of toroidal magnetization in the ground state of **D-2**, this can be still induced by applying homogeneous magnetic field $\vec{H}$ to single crystals of these compounds. This will occur when the gain of Zeeman energy due to flopping of one (μ or μ_{Cu}) magnetic sub-lattice $\Delta E_{Zee} = 2\mu_B(\vec{\mu}_{Cu} + \vec{\mu})\cdot\vec{H}$ per unit cell, will match the accompanied loss of exchange energy, $\Delta E_{exch} = \frac{\sqrt{3}-1}{4}|\tilde{J}_2|$ per unit cell. In the simplest case of $\vec{H}$ applied along the direction of magnetization on Cu ($\vec{\mu}_{Cu}$) we have the estimation $H_c = (\sqrt{3}-1)|\tilde{J}_2|/8(\mu_{Cu} + \cos\alpha\cdot\mu) = 0.37$ T, where α is the angle between $\vec{\mu}^n$ and $\vec{\mu}^n_{Cu}$ (Fig. 5b). Note that the obtained H_c is under the threshold of reversal of magnetic moments on Dy sites. The ground state arising at $H > H_c$ is shown in Fig. 6. Given the similarity of magnetic properties of **D-2** and **L-2** (Fig. 2 and 3) all conclusions about magnetic properties of **D-2** apply equally well for the **L-2** compound.

Conclusion

In conclusion, we present here heterometallic Cu^{II}/Dy^{III} 1D polymers (**L-2**, **D-2**) built from an alternation between the

trinuclear Dy_3 SMM-building blocks and chiral copper(II) *bis*-valinate complexes. The CD spectroscopy and the X-ray diffraction studies show the enantiopurity of the obtained compounds with chirogenesis of the chiral environment of the Dy_3 antiferromagnetic frustrated SMM. Comparative analysis of Gd^{III} (**D-3**) and Y^{III} (**L-1**) analogues suggests the presence of a weak antiferromagnetic interaction along the chain. We found that the ground state of the Dy_3 units in the chain is characterized by almost perfect toroidal moments which interact *via* exchange coupling with Cu ions along the chain. These systems show that using chiral building blocks is sufficient to induce polarity in the resulting system, although not necessarily chirality. Here **D-2** and **L-2** represent the first example of exchange coupling between toroidal moments. According to the calculations, a very strong toroidal magnetization can be induced in single-crystals of these compounds by applying a magnetic field at low temperature. Therefore the compounds investigated here are multiferroics of *T*–*F* type,[6c,d] where the applied homogeneous magnetic field can induce toroidal magnetization, and *vice versa*, and an applied circular magnetic field can induce a homogeneous ferromagnetic moment in the crystal. With the possibility of induced ferrotoroidicity, the Dy_3Cu polymers described here represent the first molecular-based material among the inorganic multiferroic crystals known to date.[6c,d]

Experimental section

Experimental details of synthesis and spectral characterisation are in supplementary materials. Magnetic susceptibility data were collected on powdered samples using a Quantum Design MPMS SQUID magnetometer under a 0.1 T applied magnetic field. All data were corrected for diamagnetism of the ligands estimated from Pascal's constants. Circular dichroism (CD) curves were recorded using a Chirascan™ Circular Dichroism Spectrometer as freshly prepared KBr pellets (1.0 mg of product in 100 mg of KBr). To enable comparison the spectra were normalized and corrected for baseline deviation.

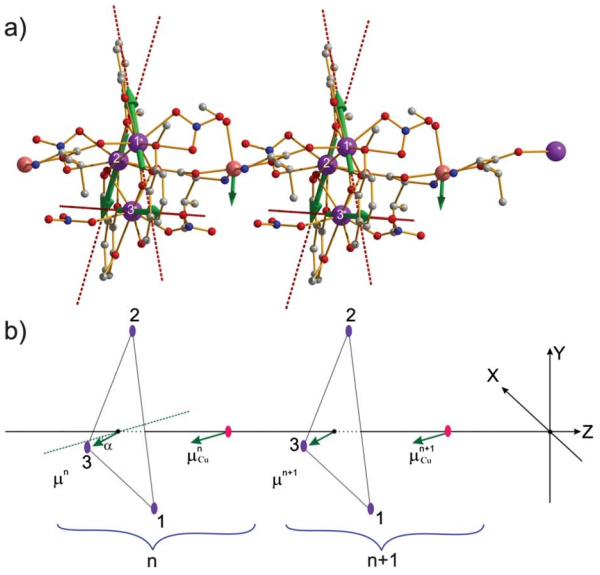

Fig. 6 Orientations of μ and μ_{Cu} along the **D-2** chain in the presence of an applied magnetic field $H > H_c$ (see the text).

X-ray analysis

Data collected on an Oxford Gemini diffractometer equipped with a CCD camera.[21a] Analytical absorption correction based on crystal shape was applied.[21b] All structures solved by direct methods using the SIR97 program[21c] and refined against F ($I > 3\sigma(I)$ using the CRYSTALS program.[21d] For all structures all non-hydrogen atoms were refined anisotropically with hydrogen atoms associated with carbon atoms placed in calculated positions and those on oxygen atoms located from difference maps and allowed to ride on the parent. Flack parameter refined for each structure to check enantiopurity.[21e]

L-2 (Dy_3Cu): $C_{69}H_{93}Cu_2Dy_6N_{11}O_{54}$ (M_r = 3042.6 g mol^{-1}); monoclinic, $P2_1$, a = 11.2309(6) Å, b = 23.818(1) Å, c = 20.393(1) Å, β = 102.308(5)°, V = 5329.8(4) Å^3, ρ = 1.896 g cm^{-3}, $F(000)$ = 2940, μ(Mo-Kα) = 4.637 mm^{-1}; T = 110 K; 23862 unique reflections (R_{int} = 0.061), refinement (on F with $I > 3\sigma(I)$): R = 0.0624, R_w = 0.0756, S = 1.06 (18342 reflections used, 1238 refined parameters), $\Delta\rho_{max}$ = 2.41 e$^-$ Å^{-3}, $\Delta\rho_{min}$ = −1.94 e$^-$ Å^{-3}, Flack parameter = −0.01(1); crystal shape: prismatic blue, 0.197 × 0.272 × 0.329 mm^3.

D-2 (Dy_3Cu): $C_{69}H_{93}Cu_2Dy_6N_{11}O_{54}$ (M_r = 3042.6 g mol^{-1}); monoclinic, $P2_1$, a = 11.2590(6) Å, b = 24.017(1) Å, c = 20.506(1) Å, β = 101.793(5)°, V = 5428.0(4) Å^3, ρ = 1.862 g cm^{-3}, $F(000)$ = 2940, μ(Mo-Kα) = 4.554 mm^{-1}; T = 110 K; 20498 unique reflections (R_{int} = 0.040), refinement (on F with $I > 3\sigma(I)$): R = 0.0542, R_w = 0.0576, S = 1.08 (14613 reflections used, 1280 refined parameters), $\Delta\rho_{max}$ = 2.16 e$^-$ Å^{-3}, $\Delta\rho_{min}$ = −1.49 e$^-$ Å^{-3}, Flack parameter = 0.96(2); crystal shape: prismatic blue, 0.162 × 0.182 × 0.299 mm^3.

D-3 (Gd_3Cu): $C_{69}H_{93}Cu_2Gd_6N_{11}O_{54}$ (M_r = 3011.1 g mol^{-1}); monoclinic, $P2_1$, a = 11.348(1) Å, b = 24.012(2) Å, c = 20.661(2) Å, β = 102.060(9)°, V = 5506.5(8) Å^3, ρ = 1.815 g cm^{-3}, $F(000)$ = 2916, μ(Mo-Kα) = 4.029 mm^{-1}; T = 110 K; 21476 unique reflections (R_{int} = 0.035), refinement (on F with $I > 3\sigma(I)$): R = 0.0639, R_w = 0.0695, S = 1.00 (15094 reflections used, 1202 refined parameters), $\Delta\rho_{max}$ = 1.91 e$^-$ Å^{-3}, $\Delta\rho_{min}$ = −1.63 e$^-$ Å^{-3}, Flack parameter = 0.97(2); crystal shape: prismatic blue, 0.192 × 0.306 × 0.396 mm^3.

L-2 (Y_3Cu): due to very weak diffraction of all tested crystals it was not possible to refine the data with anisotropic terms for non-hydrogen atoms. Nevertheless, the unit-cell parameters confirm the isostructural nature of the compound: monoclinic, $C_{69}H_{85}Cu_2Y_6N_{11}O_{54}$ (M_r = 2593.0 g mol^{-1}); $P2_1$, a = 11.242(2) Å, b = 23.756(5) Å, c = 20.528(4) Å, β = 102.49(2), V = 5352(1) Å^3; T = 110 K; Flack parameter ~ 0 (refined considering isotropic terms for non-hydrogen atoms); crystal shape: prismatic blue, 0.131 × 0.163 × 0.220 mm^3. Crystallographic data for the structures in this paper have been deposited with the Cambridge Crystallographic Data Centre as supplementary publications no. CCDC 825779–825782. Copies of the data can be obtained, free of charge, on application to CCDC, 12 Union Road, Cambridge CB2 1EZ, UK: http://www.ccdc.cam.ac.uk/cgi-bin/catreq.cgi, e-mail: data_request@ccdc.cam.ac.uk.

Acknowledgements

G. Novitchi is grateful to the EU FP-7 and AvH Foundation for financial support. L. Ungur acknowledges the research grants INPAC and Methusalem from K. U. Leuven. A. K. Powell

thanks the University of Lyon for the provision of a visiting professorship and the DFG Center for Functional Nanostructures for long term support.

Notes and references

1 (*a*) A. Werner, *Z. Anorg. Chem.*, 1893, **3**, 267; (*b*) A. Werner and A. Vilmos, *Z. Anorg. Allg. Chem.*, 1899, **21**, 145; (*c*) A. Von Zelewsky, *Stereochemistry of coordination compounds*, Vol. 3, John Wiley & Sons Inc, 1996; (*d*) H. Amouri, M. Gruselle, D. Chirality in *transition metal chemistry: molecules, supramolecular assemblies and materials*, Vol. 12, Wiley Chichester, UK, 2008.

2 D. Gatteschi, R. Sessoli, J. Villain, *Molecular Nanomagnets*, Oxford University Press, Oxford, 2006.

3 (*a*) J. M. Lehn, *Angew. Chem., Int. Ed. Engl.*, 1988, **27**, 89; (*b*) J. M. Lehn, *Angew. Chem., Int. Ed. Engl.*, 1990, **29**, 1304.

4 C. Train, M. Gruselle and M. Verdaguer, *Chem. Soc. Rev.*, 2011, **40**, 3297.

5 (*a*) L. F. Chibotaru, L. Ungur and A. Soncini, *Angew. Chem., Int. Ed.*, 2008, **47**, 4126; (*b*) L. Ungur, W. Van den Heuvel and L. F. Chibotaru, *New J. Chem.*, 2009, **33**, 1224; (*c*) J. Luzon, K. Bernot, I. J. Hewitt, C. E. Anson, A. K. Powell and R. Sessoli, *Phys. Rev. Lett.*, 2008, **100**, 247205; (*d*) J. K. Tang, I. Hewitt, N. T. Madhu, G. Chastanet, W. Wernsdorfer, C. E. Anson, C. Benelli, R. Sessoli and A. K. Powell, *Angew. Chem., Int. Ed.*, 2006, **45**, 1729; (*e*) G. Novitchi, W. Wernsdorfer, L. F. Chibotaru, J. P. Costes, C. E. Anson and A. K. Powell, *Angew. Chem., Int. Ed.*, 2009, **48**, 1614.

6 (*a*) L. D. Barron, *J. Am. Chem. Soc.*, 1985, **108**, 5539; (*b*) B. M. Tanygin, *Phys. B*, 2011, **406**, 3423; (*c*) H. Schmidt, *J. Phys.: Condens. Matter*, 2008, **20**, 434201; (*d*) T. Kaelberer, V. A. Fedotov, N. Papasimakis, D. P. Tsai and N. I. Zheludev, *Science*, 2010, **330**, 1510.

7 (*a*) J. P. Costes, F. Dahan and F. Nicodeme, *Inorg. Chem.*, 2001, **40**, 5285; (*b*) X. P. Yang, R. A. Jones and M. J. Wiester, *Dalton Trans.*, 2004, 1787.

8 R. D. Shannon, *Acta Crystallogr., Sect. A: Cryst. Phys., Diffr., Theor. Gen. Crystallogr.*, 1976, **32**, 751.

9 V. Schurig and U. Leyrer, *Tetrahedron: Asymmetry*, 1990, **1**, 865.

10 (*a*) R. Andreu, I. Malfant, P. G. Lacroix, P. Cassoux, K. Roque, E. Manoury, J.-C. Daran and G. A. Balavoine, *C.R. Acad. Sci. Paris série II*, 1999, 329–340; (*b*) K. S. Jeong, B. H. Lee, Q. Li, S. B. Choi, J. Kim and N. Jeong, *CrystEngComm*, 2011, **13**, 1277–1279.

11 J. J. Borras-Almenar, J. M. Clemente-Juan, E. Coronado and B. S. Tsukerblat, *J. Comput. Chem.*, 2001, **22**, 985.

12 (*a*) A. Q. Wu, G. H. Guo, C. Yang, F. K. Zheng, X. Liu, G. C. Guo, J. S. Huang, Z. C. Dong and Y. Takano, *Eur. J. Inorg. Chem.*, 2005, 1947; (*b*) X. M. Chen, Y. L. Wu, Y. Y. Yang, S. M. J. Aubin and D. N. Hendrickson, *Inorg. Chem.*, 1998, **37**, 6186; (*c*) R. Baggio, M. T. Garland, Y. Moreno, O. Pena, M. Perec and E. Spodine, *J. Chem. Soc., Dalton Trans.*, 2000, 2061; (*d*) R. Calvo, R. E. Rapp, E. Chagas, R. P. Sartoris, R. Baggio, M. T. Garland and M. Perec, *Inorg. Chem.*, 2008, **47**, 10389; (*e*) S. C. Manna, S. Konar, E. Zangrando, J. Ribas and N. Ray Chaudhuri, *Polyhedron*, 2007, **26**, 2507.

13 C. Benelli and D. Gatteschi, *Chem. Rev.*, 2002, **102**, 2369.

14 (*a*) I. J. Hewitt, J. Tang, N. T. Madhu, C. Anson, Y. Lan, J. Luzon, M. Etienne, R. Sessoli and A. K. Powell, *Angew. Chem., Int. Ed.*, 2010, **49**, 6352; (*b*) I. J. Hewitt, Y. Lan, C. E. Anson, J. Luzon, R. Sessoli and A. K. Powell, *Chem. Commun.*, 2009, 6765.

15 (*a*) F. Aquilante, L. De Vico, N. Ferre, G. Ghigo, P. A. Malmqvist, P. Neograd y, T. B. Pedersen, M. Pitonak, M. Reiher, B. O. Roos, L. Serrano-Andres, M. Urban, V. Veryazov, R. Lindh, *J. of Comp. Chem.*, **31**, p. 224; (*b*) L. F. Chibotaru, L. Ungur, C. Aronica, H. Elmoll, G. Pilet and D. Luneau, *J. Am. Chem. Soc.*, 2008, **130**, 12445; (*c*) D. Visinescu, A. M. Madalan, M. Andruh, C. Duhayon, J. P. Sutter, L. Ungur, W. Van den Heuvel and L. F. Chibotaru, *Chem.–Eur. J.*, 2009, **15**, 11808.

16 M. E. Lines, *J. Chem. Phys.*, 1971, **55**, 2977.

17 J. Long, F. Habib, P.-H. Lin, I. Korobkov, G. Enright, L. Ungur, W. Wernsdorfer, L. F. Chibotaru and M. Murugesu, *J. Am. Chem. Soc.*, 2011, **133**, 5319.

18 P.-H. Lin, I. Korobkov, W. Wernsdorfer, L. Ungur, L. F. Chibotaru and M. Murugesu, *Eur. J. Inorg. Chem.*, 2011, 1535.

19 W. Van den Heuvel and L. F. Chibotaru, *Phys. Rev. B*, 2010, **77**, 220406.

20 A. Soncini and L. F. Chibotaru, *Phys. Rev. B: Condens. Matter Mater. Phys.*, 2008, **77**, 220406(R).

21 (*a*) CrysAlisPro Version 1.171.34.40 (release 27-08-2010 CrysAlis171.NET); Oxford Diffraction Ltd; (*b*) CrysAlisPro, O.D.L. Version 1.171.34.40 (release 27-08-2010 CrysAlis171.NET)(compiled Aug 27 2010,11:50 : 40). Analytical numeric absorption correction using a multifaceted crystal model based on expressions derived by R. C. Clark and J. S. Reid, *Acta Crystallogr., Sect. A: Found. Crystallogr.*, 1995, **51**, 887–897; (*c*) G. Cascarano, A. Altomare, C. Giacovazzo, A. Guagliardi, A. G. G. Moliterni, D. Siliqi, M. C. Burla, G. Polidori and M. Camalli, *Acta Cryst.*, 1966, **A52**; (*d*) D. Watkin; C. Prout; J. Carruthers; P. Betteridge, *CRISTAL Issue 11*. In Chemical Crystallography Laboratory: Oxford, UK: 1999; (*e*) H. Flack, *Acta Crystallogr., Sect. A: Found. Crystallogr.*, 1983, **39**, 876–881.

